

Mefenamic Acid Anti-Inflammatory Drug: Probing Its Polymorphs by Vibrational (IR and Raman) and Solid-State NMR Spectroscopies

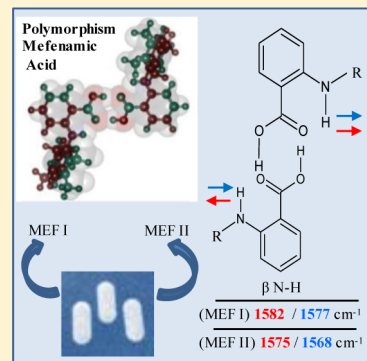
Vanessa R. R. Cunha,[†] Celly M. S. Izumi,^{†,||} Philippe A. D. Petersen,[‡] Alviclé Magalhães,[§] Marcia L. A. Temperini,[†] Helena M. Petrilli,[‡] and Vera R. L. Constantino^{*,†}

[†]Departamento de Química Fundamental, Instituto de Química, Universidade de São Paulo, Av. Prof. Lineu Prestes 748, CEP 05508-000, São Paulo-SP, Brazil

[‡]Departamento de Física dos Materiais e Mecânica, Instituto de Física, Universidade de São Paulo, CEP 05315-970, São Paulo-SP, Brazil

[§]Departamento de Química Inorgânica, Instituto de Química, Universidade Estadual de Campinas, CEP 13083-970, Campinas-SP, Brazil

ABSTRACT: This work deals with the spectroscopic (supported by quantum chemistry calculations), structural, and morphological characterization of mefenamic acid (2-[2,3-(dimethylphenyl)amino] benzoic acid) polymorphs, known as forms I and II. Polymorph I was obtained by recrystallization in ethanol, while form II was reached by heating form I up to 175 °C, to promote the solid phase transition. Experimental and theoretical vibrational band assignments were performed considering the presence of centrosymmetric dimers. Besides band shifts in the 3345–3310 cm⁻¹ range, important vibrational modes to distinguish the polymorphs are related to out-of-phase and in-phase N–H bending at 1582 (Raman)/1577 (IR) cm⁻¹ and 1575 (Raman)/1568 (IR) cm⁻¹ for forms I and II, respectively. In IR spectra, bands assigned to N–H bending out of plane are observed at 626 and 575 cm⁻¹ for polymorphs I and II, respectively. Solid-state ¹³C NMR spectra pointed out distinct chemical shifts for the dimethylphenyl group: 135.8 to 127.6 ppm (carbon bonded to N) and 139.4 to 143.3 ppm (carbon bonded to methyl group) for forms I and II, respectively.

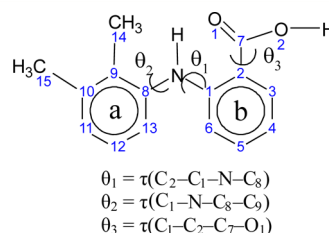


INTRODUCTION

Polymorphism is a well-known feature present in solid materials. In the pharmaceutical industry, its importance relies on the distinct physicochemical and mechanical properties that the different forms can exhibit such as apparent solubility, dissolution rate, chemical stability, bioavailability, and processability.^{1–4} Therefore, it is crucial to deeply explore solid-state characterization techniques in order to identify drugs which present two or more crystalline phases.⁵

Mefenamic acid or 2-[2,3-(dimethylphenyl)amino] benzoic acid, a derivative of fenamic acid, is a potent inhibitor of prostaglandin synthesis, which is closely related to inflammatory processes.^{6,7} It is indicated, for example, in cases of muscle, trauma, and dental pain, headaches, premenstrual syndrome, and postoperative surgeries.⁸ Also, mefenamic acid has been shown therapeutic effects in neurodegeneration disease (Alzheimer's) and anticancer agents (particularly colon and liver cancer cell lines).^{9–11} The molecular structure of mefenamic acid is shown in Figure 1.^{12–15}

The molecular structure of mefenamic acid presents coplanarity between the carboxylic group and the nitrogen atom of the aromatic ring. The sum of the angles of the three linkages around the nitrogen is almost 360°, indicating that hybridization of the nitrogen atom can be considered as sp² type. Molecular mechanics calculations have shown that the lone pair on the nitrogen atom is in resonance with the



$$\begin{aligned}\theta_1 &= \tau(C_2-C_1-N-C_8) \\ \theta_2 &= \tau(C_1-N-C_8-C_9) \\ \theta_3 &= \tau(C_1-C_2-C_7-O_1)\end{aligned}$$

Figure 1. 2D schematic representation of mefenamic acid structure, where $\tau(C_1, C_2, \dots)$ represents the dihedral torsion.

aromatic rings.¹² The resonance interactions and the hydrogen bonds between the oxygen of the carboxylic unit and the hydrogen of the amine group have been suggested to be, in part, responsible for the molecular coplanarity.¹³

In the solid state, mefenamic acid can be crystallized in two forms, designated as form I (MEF I) and form II (MEF II). The crystalline structure of the stable MEF I form was solved by McConnell and Company.¹⁴ The metastable structure, MEF II, was only resolved by single crystal X-ray diffraction in 2006 by Lee et al.¹⁵ In both polymorphs, two molecules interact

Received: January 28, 2014

Revised: March 17, 2014

Published: March 24, 2014



through intermolecular hydrogen bonds via carboxylic groups producing dimers. The difference involving MEF I and MEF II structures is on the torsion angle θ_2 between the aromatic rings (Figure 1). The dimethylphenyl ring twist reduces the energy of the crystal lattice.¹⁶ Very recently, Seethalekshmi and Row¹⁷ have reported the isolation of a new metastable polymorph of mefenamic acid.

Polymorph MEF I is obtained, for example, from solutions of acetone or ethanol, while MEF II can be isolated by recrystallization in dimethylformamide (DMF).¹⁸ A phase transition from form I to form II in the solid state is observed at about 160–190 °C (the variation in the transition temperature is related to the heating rate).¹⁹ Another process to transform MEF I into MEF II is through the compression of the solid.²⁰

Despite the pharmaceutical importance of mefenamic acid polymorphism, a complete spectroscopic characterization of its polymorphs has not yet been performed. Although Kruszynski et al.²¹ have already compared the experimental and calculated vibrational spectrum of mefenamic acid, only the dimer of polymorph I was considered. In addition, the differences in the infrared and Raman spectra, due to the presence of the centrosymmetric dimer, were not highlighted. Furthermore, a few numbers of works have employed vibrational (Raman and IR) spectroscopy to distinguish the monomer and dimer conformations of small molecules like formic acid,²² pivalic acid,²³ pyrrole acid,²⁴ toluic acid,²⁵ (S)-(-) perilllic acid,²⁶ and fluoroisonicotinic acid.²⁷ In this regard, only two papers took into account those techniques to identify the differences between the monomer and the dimer of molecules with pharmacological activities, such as the anti-inflammatory ibuprofen²⁸ and the antioxidant cinnamic acid.²⁹

The aim of the present work is to characterize forms I and II of mefenamic acid using valuable tools for molecular structural investigation: vibrational (Raman and infrared) and solid-state ¹³C nuclear magnetic resonance (NMR) spectroscopies and computational calculations in the framework of density functional theory (DFT). Considering that spectroscopic techniques are routinely employed in academic and industrial laboratories, an accurate attribution of the spectral signatures of polymorph forms is a topic of pronounced concern.

■ EXPERIMENTAL AND THEORETICAL METHODS

Preparation of Polymorphs I and II of Mefenamic Acid. In the preparation of mefenamic acid, initially 40 mL of ethanol was saturated with an excess of mefenamic acid at room temperature. The suspension was kept under stirring at 60 °C for about 6 h, as described in the literature.³⁰ After the complete dissolution of mefenamic acid in the solvent, the solution was cooled to room temperature and stored in a refrigerator for 1 day to enhance the precipitate amount. The solid (MEF I) was filtered, washed with deionized water, and dried under reduced pressure in a desiccator containing silica gel.

MEF II solid was obtained by heating the MEF I sample from room temperature to 175 °C in the thermoanalyzer equipment as described in the literature.³¹ The phase transition was promoted under a flow of N₂ gas (50 mL/min) using a heating rate of 10 °C/min and alumina crucible.

Experimental Characterization. X-ray diffraction (XRD) patterns of powdered samples were recorded on a Rigaku diffractometer, model Miniflex, using Cu K α radiation (1.541 Å, 30 kV, 15 mA, scan step of 0.03°) and a Ni filter.

Simultaneous thermogravimetric analysis and differential scanning calorimetry (TGA-DSC) were recorded on a Netzsch thermoanalyzer model TGA/DSC 490 PC Luxx, using a heating rate of 10 °C/min and under N₂ gas flow of 50 mL/min.

Field emission scanning electron microscopy (FE-SEM) images were obtained with a JEOL microscope, model JSM-7000F, at the Instituto de Química (Universidade de São Paulo - USP). The uncoated MEF I and MEF II samples were placed over a copper tape.

Fourier transform Raman (FT-Raman) spectra were recorded in a FT-Raman Bruker RFS-100/S spectrometer using 1064 nm exciting radiation (Nd:YAG laser Coherent Compass 1064-500N) and a Ge detector. Laser power was kept below 20 mW to avoid sample degradation.

Fourier transform infrared (FTIR) spectra of samples diluted in KBr were recorded on a Bomen spectrophotometer, model MB-102, with a coupled diffuse reflectance accessory (Pike Technologies, Inc.) in the range 4000–400 cm⁻¹ and acquisition step of 1 cm⁻¹.

Solid-state NMR data were obtained in a Bruker Avance II+ NMR spectrometer 300 MHz for ¹H and 75 MHz for ¹³C. The signals were acquired at room temperature using CP/MAS, spinning a 4 mm rotor at 10 kHz, using 4 ms of contact time for cross-polarization, tppm sequence for ¹H decoupling, and 1 s of recycle delay. The FIDs were processed using an exponential window function with 30 Hz of line broadening. The ¹³C chemical shifts were calibrated using DSS (4,4-dimethyl-4-silapentane-1-sulfonic acid) as a reference.

Computational Calculations. The geometry of the conformers of the mefenamic acid dimers was optimized at the B3LYP/6-311++G(d,p) levels of theory,^{32,33} in the framework of the DFT. Isotropic chemical shifts for MEF I and MEF II were calculated in vacuum using the tetramethylsilane molecule (TMS) as the reference to obtain the ¹³C NMR chemical shifts of the dimers. Theoretical calculations were performed with the standard Gaussian 03 package gauge including atomic orbitals (GIAO) method.^{34,35} The equivalence of the monomers forming the complexes was assumed: for each kind of dimer, two associated monomers are related by the center of inversion. Calculated wavenumber values were scaled down by a single factor (0.9679)³⁶ in order to correct anharmonicity effects in the simulation of the vibrational spectra. Assignments of mefenamic acid vibrational (IR and Raman) modes were obtained by visual inspection of the displacement vectors. The procedure adopted here is analogous (but with an improved basis set) to that used by some of us.³⁷ As mentioned by Tzeli et al.,³⁸ the hydrogen bonds can be well described within the theoretical level of calculations applied here.

■ RESULTS AND DISCUSSION

XRD patterns of MEF I and MEF II compounds are shown in Figure 2. The results are in good agreement with those previously reported in the literature.^{30,31,39–44} Therefore, the isolation of both compounds is confirmed, through the methods used here. For the main peaks (that characterize the polymorphs), the 2 θ values and their corresponding interplanar distances are shown in Table 1.

The crystal morphologies of the pharmaceutical compounds were examined by FE-SEM (Figure 3). There is a substantial difference in the crystal habits of the two polymorphs. MEF I crystals, obtained from ethanol solution, show needle-shaped

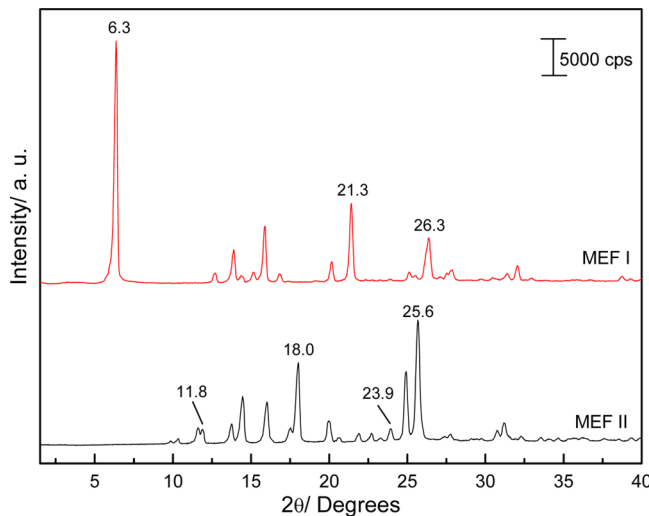


Figure 2. XRD patterns of MEF I and MEF II samples.

Table 1. Main Interplanar Distances (d_{hkl}) and 2θ ($\lambda = 1.54$ Å) of MEF I and MEF II Samples Obtained from XRD Data

MEF I		MEF II	
2θ	d (Å)	2θ	d (Å)
6.36	14.0	11.8	7.49
21.3	4.17	18.0	4.92
26.3	3.38	23.9	3.72
		25.6	3.48

platelets, as observed for other MEF I samples,^{30,45} with approximately 510 μm in length and 20 μm in width. MEF II particles are smaller and have about 60 μm in length and 17 μm in width. Cube-shaped particles were also observed for MEF II crystals obtained from DMF solution.³⁰ Particles of the metastable form II obtained by phase transition at 175 °C contain interesting small holes with a diameter measuring ca. 5 μm (cf. inset in Figure 3).

Figure 4 shows the TGA, DTG, and DSC curves of the MEF I form. Endothermic peaks are observed at 181 and 233 °C. These temperatures are, respectively, related to the phase transition of MEF I to the metastable MEF II form, and the melting point of MEF II. These values are coherent with those ones reported in the literature for mefenamic acid.^{31,40,42,46} The polymorphs can reversibly be transformed one into another by

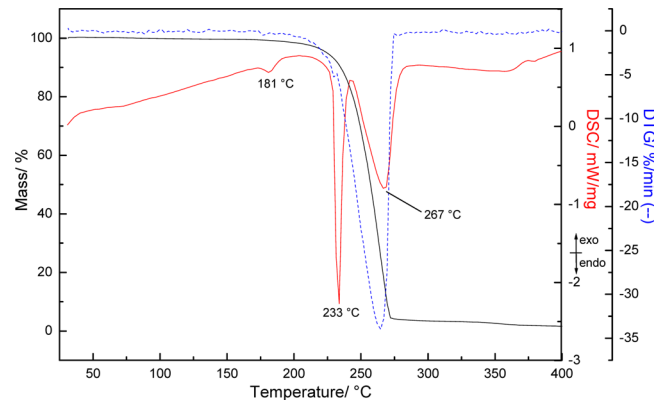


Figure 4. TGA-DTG-DSC curves of MEF I form.

heating or cooling the forms. Thus, they are examples of enantiotropes.⁴⁷ Additionally, the endothermic event at 267 °C, after the melting process of MEF II, is associated with the molecule decomposition. XRD patterns, thermal analysis data, and morphological aspects of the crystals confirm the identity of both samples (polymorphs I and II) isolated in this work.

The obtained optimized MEF I and MEF II structural parameters are shown in Table 2. The most relevant difference between MEF I and MEF II is the angle θ_2 , but also some changes are seen in θ_1 and θ_3 . These three angles are responsible for the distinct packing of the polymorphs.

The simulated structures (calculated at the B3LYP/6311+G(d,p) level of theory) of the mefenamic acid dimers can be seen in Figure 5. A very good agreement between the theoretical and experimental values available in the literature can be seen in Table 2. Jabeen et al.⁴⁸ reported the O₁···H–N bond angle equal to 138.52 Å and the C₁–N–C₈–C₉ torsion angle of –137.07°, which are different from the results obtained in this work. Our calculated values are in good agreement with the experimental data. The difference between the calculated values can be attributed to the fact that only the monomer was considered by them, which highlights the importance of the interactions within the dimer.

FTIR spectroscopy has been qualitatively used by several authors^{19,49,50} to identify the two polymorphs of mefenamic acid. However, there is practically no information concerning the relation among the spectral profiles, the molecular structures, and the arrangement of the molecules in the crystal. Hence, the vibrational analysis has not acutely been used to

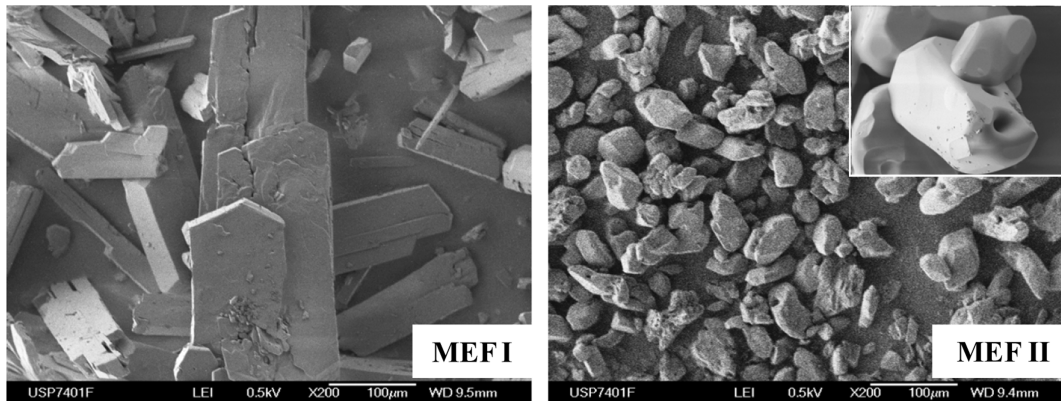


Figure 3. FE-SEM images of MEF I and MEF II samples (amplification: ×200).

Table 2. Bond Lengths (\AA), Bond Angles (deg), and Torsion Angles (deg) for the Most Stable Conformations of MEF I and MEF II, Calculated at the B3LYP/6-311++G(d,p) Level of Theory

parameter	MEF I		MEF II	
	calculated	experimental ¹¹	calculated	experimental ¹²
Bond Lengths				
C ₁ –N	1.371	1.364	1.370	1.396
C ₈ –N	1.421	1.412	1.428	1.434
C ₇ –O ₁	1.244	1.232	1.244	1.238
C–O	1.325	1.318	1.326	1.317
O–H···O ₁ (H–O)	1.679	1.685	1.677	1.699
O–H···O ₁ (O–O)	2.676	2.655	2.674	2.639
C ₇ –O ₁ ···H–N (O–N)	2.680	2.636	2.685	2.666
C ₇ –O ₁ ···H–N (H–O)	1.860	1.892	1.882	1.873
Bond Angles				
O ₁ ···H–N	135.5	135.3	133.7	136.1
C ₁ –N–C ₈	127.1	127.3	125.5	124.4
N–C ₈ –C ₉	119.5	118.8	121.1	119.5
Torsion Angles				
$\theta_1 = \tau(C_2-C_1-N-C_8)$	-170.8	-179.3	-177.4	-177.8
$\theta_2 = \tau(C_1-N-C_8-C_9)$	-129.5	-120.0	-77.7	-71.7
$\theta_3 = \tau(C_1-C_2-C_7-O_1)$	-2.63	-1.7	2.54	-0.43

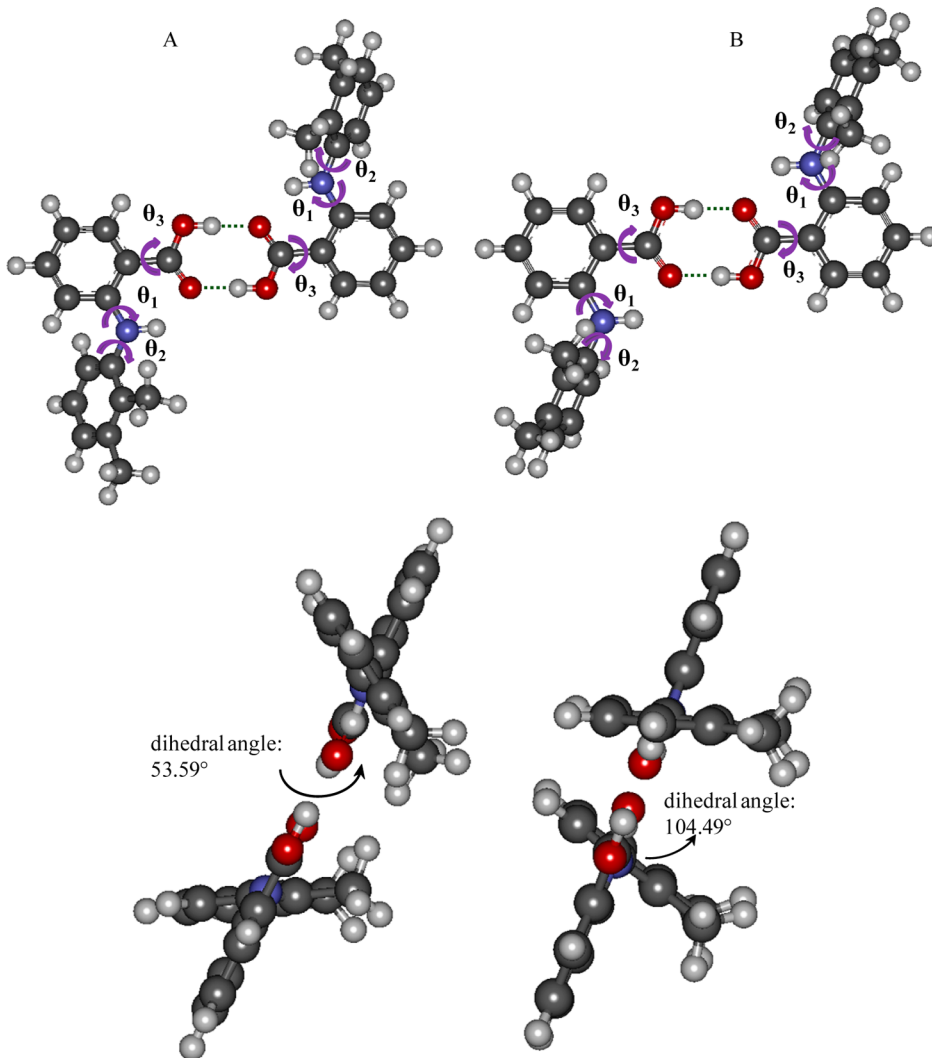


Figure 5. Optimized structures of mefenamic acid polymorphs and the dihedral angle between the two aromatic rings: (A) MEF I; (B) MEF II.

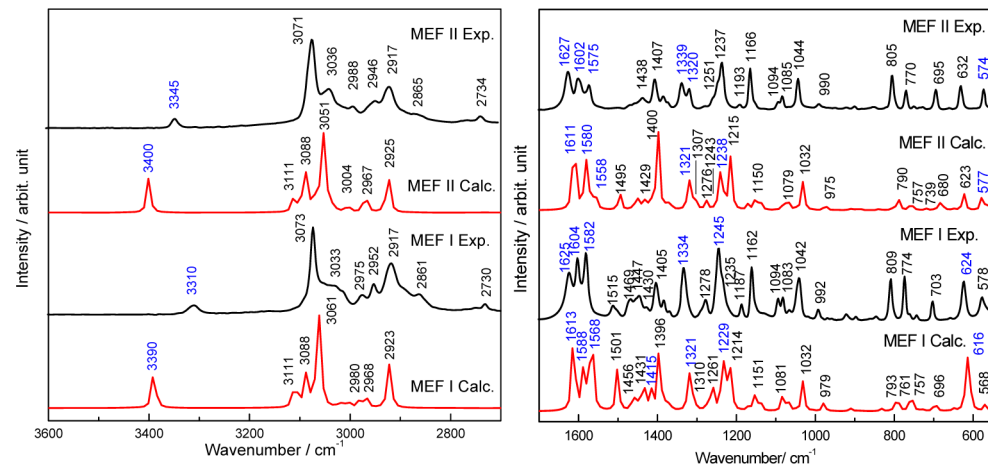


Figure 6. Experimental (black line, thin) and calculated (red line, thick) FT-Raman spectra of MEF I and MEF II samples ($\lambda_0 = 1064$ nm). The blue labeled frequencies assign the main differences among the two forms.

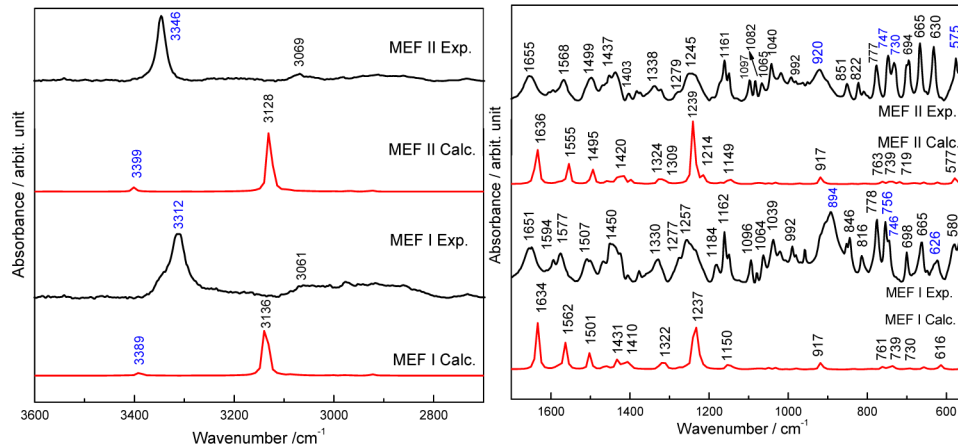


Figure 7. Experimental (black line) and calculated (red lines) FTIR spectra of MEF I and MEF II samples. The blue labeled frequencies assign the main differences among the two forms.

discriminate the mefenamic acid polymorphs. In order to improve this issue (or knowledge), Raman and IR spectra of MEF I and MEF II were obtained and an assignment of the bands was done on the basis of the DFT method.⁵¹ The equivalence of monomers forming complexes was assumed: for each kind of dimer, two associated monomers are related by a center of inversion over the eight-membered ring formed by the two carboxyl groups.

The FT-Raman and FTIR spectra of MEF I and MEF II are shown in Figures 6 and 7, respectively. Experimental and theoretical wavenumbers and the corresponding vibrational mode assignments are presented in Table 3. Our vibrational analysis has considered the differences between the bands in Raman and infrared spectra owing to the existence of centrosymmetric dimers. This kind of analysis was not contemplated in previous studies where DFT calculations were used to investigate the vibrational properties of the MEF I dimer,²¹ or the properties of the MEF I and MEF II monomers.⁴⁸

The high wavenumber region in the FT-Raman (Figure 6) and FTIR (Figure 7) spectra bands can be used to distinguish the polymorph forms. This is the case of the strong bands in Raman and IR spectra at 3310 (Raman)/3312 (IR) for MEF I and 3345/3346 cm⁻¹ for MEF II. These bands are assigned to N–H stretching modes shown in Scheme 1a and b. These

frequencies are smaller than that observed in the ν N–H of diphenylamine (3433 cm⁻¹).⁵² since as it can be seen in Figure 5, N–H groups are hydrogen bonded to the carboxyl group in mefenamic acid. The smaller wavenumber observed for the N–H stretching of MEF I suggests a stronger hydrogen bond interaction between the carboxylic groups when compared to MEF II. This is confirmed by the calculated structural parameters reported in Table 2, where the distance C₇–O₁…H–N (H–O) is shorter for MEF I. The calculated wavenumber values are not matching very satisfactorily the experimental ones due to the higher anharmonicity of the vibrational modes presented in this region (ν O–H and ν C–H).

FT-IR spectra of MEF I and MEF II dimers show very weak bands at 3061 and 3069 cm⁻¹, respectively, attributed to the ν O–H out-of-phase mode (Scheme 1c), while the Raman spectra present medium intensity bands at 3033 and 3036 cm⁻¹, assigned to the ν O–H in phase mode (Scheme 1d). However, Jabeen et al.⁴⁰ reported an inverted attribution to the stretching of the O–H (3528 cm⁻¹) and N–H (3296 cm⁻¹) groups. This difference can be related to the fact that the authors have considered the monomeric gas phase molecule and used another basis set cc-pVDZ in the DFT calculations.

Kruszynski et al.²¹ performed theoretical calculations for the vibrational frequencies but only considering a monomer and a

Table 3. Raman and IR Wavenumbers (in cm^{-1}) of MEF I and MEF II in the Solid State, Calculated Vibrational Wavenumbers (in cm^{-1}), and a Tentative Assignment^a

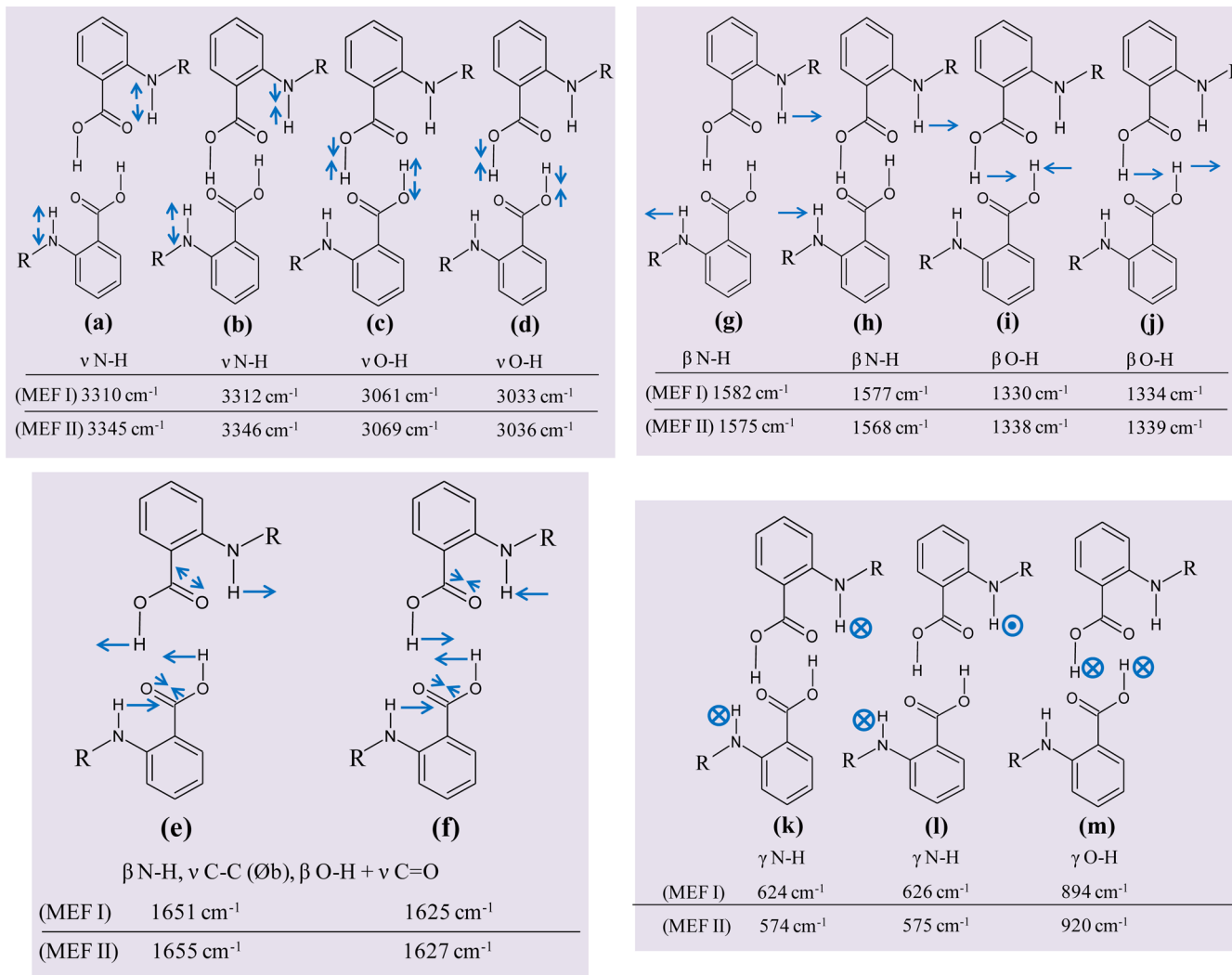
	MEF I			MEF II		
	Raman	IR	calculated	Raman	IR	calculated
3310	3312	3389	3390	3345	3346	3400
	3061	3136		3069		3399
3073		3111				3128
	3033	3088	3071			3111
2975	3061	3036	3021			3088
	2980	2988				3051
2952	2968	2946				3004
2917	2923	2917				2967
2861	2730	2865	2734			2925
						ν_{asCH_3} (C15)
very low	1651	1634				ν_{asCH_3} (C14, C15)
1625	very low	1613	1627	1655	1636	
1604		1588	1602	low	1611	$\beta\text{N}-\text{H}, \nu_{\text{C}-\text{C}}(\text{O}\text{b}), \beta\text{O}-\text{H} + \nu_{\text{C}=\text{O}}$ (e)
1582	low	1568	1575	low	1580	$\beta\text{N}-\text{H}, \nu_{\text{C}-\text{C}}(\text{O}\text{a} \text{ and } \text{O}\text{b}), \beta\text{O}-\text{H} + \nu_{\text{C}=\text{O}}$ (f)
low	1577	1562			1558	$\beta\text{N}-\text{H} (\text{g}), \nu_{\text{C}-\text{C}} (\text{O}\text{a} \text{ and } \text{O}\text{b})$
					1555	$\beta\text{N}-\text{H} (\text{h}), \nu_{\text{C}-\text{C}} (\text{O}\text{a} \text{ and } \text{O}\text{b})$
					1496	$\nu_{\text{C}-\text{C}} (\text{O}\text{b}), \beta\text{N}-\text{H} (\text{g})$
					1495	$\nu_{\text{C}-\text{C}} (\text{O}\text{b}), \beta\text{N}-\text{H} (\text{h})$
					1495	$\nu_{\text{C}-\text{C}} (\text{O}\text{b}), \beta\text{N}-\text{H} (\text{h})$
1515	1507	1501.3	1501.1	1438		1429
					1437	$\beta\text{N}-\text{H}, \nu_{\text{C}-\text{C}} (\text{O}\text{a} \text{ and } \text{O}\text{b}), \beta\text{O}-\text{H} + \nu_{\text{C}=\text{O}}$ (e), δCH_3
1447	1450	1431				$\beta\text{N}-\text{H}, \beta_{\text{C}-\text{H}} (\text{O}\text{a} \text{ and } \text{O}\text{b}), \delta\text{CH}_3$
1430sh	inactive		1415			$\beta\text{N}-\text{H}, \nu_{\text{C}-\text{C}} (\text{O}\text{a} \text{ and } \text{O}\text{b}), \beta\text{O}-\text{H}$ (i)
1405	1335–1330		1396	1407	1403 very low	$\beta\text{N}-\text{H}, \beta_{\text{C}-\text{H}} (\text{O}\text{a}, \text{O}\text{b}), \beta\text{O}-\text{H}$ (j) + $\nu_{\text{C}=\text{O}}, \delta\text{CH}_3$
1334		1322	1321	1339	1338–1340	$\beta\text{N}-\text{H}, \nu_{\text{C}-\text{C}} (\text{O}\text{a} \text{ and } \text{O}\text{b}), \beta\text{O}-\text{H} + \nu_{\text{C}=\text{O}}$ (e)
					1324	$\beta\text{O}-\text{H} (\text{i}), \nu_{\text{C}-\text{C}} (\text{O}\text{b})$
					1321	$\beta\text{C}-\text{H}$ in phase (Ob), $\nu_{\text{C}1-\text{N}}, \gamma_{\text{N}-\text{H}}$ (k)
					1309	$\beta\text{C}-\text{H}$ in phase (Ob), $\nu_{\text{C}1-\text{N}}, \gamma_{\text{N}-\text{H}}$ (l)
1278	1277	1261	1310 (very low)	1320	1279	$\beta\text{C}-\text{H}$ in phase ($\text{O}\text{a}, \text{O}\text{b}$), $\nu_{\text{C}1-\text{N}}, \gamma_{\text{N}-\text{H}}$ (k)
	~1257 (broad)	1237	1229	1251sh	~1245 (broad)	$\beta\text{O}-\text{H}, \beta_{\text{C}-\text{H}}$ in phase ($\text{O}\text{a}, \text{O}\text{b}$), $\nu_{\text{C}-\text{COOH}}$
1245				1237		$\beta\text{O}-\text{H} (\text{j}), \beta_{\text{C}-\text{H}}$ in phase ($\text{O}\text{a}, \text{O}\text{b}$)
1235sh						$\beta\text{N}-\text{H} (\text{j}), \beta_{\text{C}-\text{H}}$ in phase ($\text{O}\text{a}, \text{O}\text{b}$)
1162	1162	1151				$\beta\text{C}-\text{H}$ in phase ($\text{O}\text{a}, \text{O}\text{b}$)
1094	1096	1081				$\beta\text{C}-\text{H}$ in phase ($\text{O}\text{a}, \text{O}\text{b}$), $\nu_{\text{C}-\text{COOH}}$
1083						$\beta\text{C}-\text{H}$ in phase ($\text{O}\text{a}, \text{O}\text{b}$), ν_{CH_3}

Table 3. continued

	MEF I			MEF II		
	Raman	IR	calculated	Raman	IR	calculated
1042	1039	1032	1044	1040	1032	ν C—C (O _b)
992	992	979	990	992	975	wCH ₃
	894 (broad)	917	920 (broad)		917	γ O—H (m)
809		793	805		790	γ C—H in phase (O _a), δ C—C—C in phase (O _b), β COOH
	778	761	777		763	γ C—H in phase (O _a)
774	756	757	770		757	γ C—H in phase (O _a), β COOH
	746	739	747		739	γ C—H in phase (O _b)
703	698	696	695	730	719	γ C—H in phase (O _a), γ CH ₃ (C14)
	665				680	C—C—C in phase puckering (O _a , O _b), γ CH ₃ (C14, C15)
	624	626	616	632	623	δ C—C—C in phase (O _b), C—C—C in phase puckering (O _a , O _b), γ N—H (k)
	626	615	574	575	577	γ N—H (k)
578	580	568	575		576	γ N—H (l)
						δ C—C—C in phase (O _a , O _b)

^aThe selected values of wavenumbers (cm^{-1}) are multiplied by 0.9679, according to the computational calculations description. O_a, O_b = phenyl group labeled according to Figure 1, ν = stretching, δ = bending, β = bending in plane, γ = bending out of plane, r = rocking, w = wagging, s = symmetric, as = antisymmetric, sh = shoulder, dimer; labeled according to Scheme 1.

Scheme 1. Schematic Representation of Some Vibrational Modes of Mefenamic Acid Polymorphs



dimer of the MEF I form. They found different wavenumbers in the cases of monomer (1667 cm^{-1}) and dimer (1634 cm^{-1}), attributed to the $\nu\text{ C=O}$ and $\delta\text{ N-H}$. The presently obtained 1634 cm^{-1} calculated values agree with the dimer result of Kruszynski et al. Nevertheless, the C=O stretching is also found in other frequencies and other vibrational modes were also observed here at 1634 cm^{-1} (see Table 3).

In the medium region in the IR spectra, MEF I and MEF II bands at 1651 and 1655 cm^{-1} , respectively, are intense in the IR spectra and correspond to the vibrational mode shown in Scheme 1e. In the Raman spectra of both polymorphs, bands at 1627 – 1625 cm^{-1} are observed, which are assigned to the motion illustrated in Scheme 1f. These bands at around 1650 cm^{-1} (IR) and 1620 cm^{-1} (Raman) exhibit also contributions from $\beta\text{ O-H}$ and $\nu\text{ C-C}(\emptyset\text{b})$ groups. On the other hand, Jabeen et al.⁴⁸ assigned, for both forms, the bands at 1624 – 1627 cm^{-1} in the Raman spectra to the benzene ring stretching.

Theoretical data can provide a better attribution of the intense bands in the 1700 – 1550 cm^{-1} region, and expose the differences between the Raman and IR spectra due to the presence of centrosymmetric dimers. The shift of about 7 cm^{-1} (1582 and 1575 cm^{-1} for MEF I and II, respectively) between the forms, regarding the out-of-phase (Scheme 1g) and in-phase (Scheme 1h) N-H bending (and also the stretching of

the aromatic rings) in the 1585 – 1560 cm^{-1} region, has shown another marker to differentiate MEF I and MEF II.

The calculated wavenumbers assigned to the $\beta\text{N-H}$ (Scheme 1g and h) and $\nu\text{C-C}$ of $\emptyset\text{b}$ at 1582 cm^{-1} (MEF I) and 1575 cm^{-1} (MEF II) can also be used to distinguish the polymorphs. A closer inspection at the calculated vibrational spectra of MEF I showed two bands very close in energy (1501.3 and 1501.1 cm^{-1}), the first being active in the IR and the second in the Raman, which are not observed in MEF II. In the experimental spectra, the Raman band at 1515 cm^{-1} present in MEF I is absent in the MEF II spectrum, whereas the IR band of MEF II at 1499 cm^{-1} is absent in the MEF I spectrum. Other bands close in energy which could be found only for MEF II are at 1495 and 1496 cm^{-1} . The calculation data showed that the Raman intensity is lower than that in the IR spectrum (in fact, the experimental Raman spectrum of MEF II does not show bands in the 1500 cm^{-1} region).

The O-H bending in phase (Scheme 1i) and out of phase (Scheme 1j), shown by the bands in the 1330 – 1340 cm^{-1} region, present another remarkable difference between forms I and II, which only exists due to the dimeric structure.

According to DFT calculations, the vibrational mode comprised by the $\beta\text{C-H}$ in phase ($\emptyset\text{b}$), $\nu\text{C1-N}$, and $\gamma\text{N-H}$ (Scheme 1k and l) arises from the dimeric nature of mefenamic

acid in the crystal. However, bands in the 1310 cm^{-1} region associated with these modes are not straightforwardly visualized in the experimental spectra. Calculations also show a significant difference between the polymorphs when considering modes involving the $\nu\text{ C-COOH}$ vibration. The expected alterations in the $1240\text{--}1260\text{ cm}^{-1}$ region are indeed observed in the experimental Raman and IR spectra (see Table 3).

Interestingly, the band associated with the $\gamma\text{ O-H}$ mode of dimeric units (Scheme 1m) is observed in distinct positions: at 894 cm^{-1} for MEF I and at 920 cm^{-1} in the case of MEF II. The MEF I Raman band at 703 cm^{-1} assigned to C-C-C in-phase puckering ($\varnothing\text{a}, \varnothing\text{b}$) + γCH_3 (C14, C15) is shifted to 695 cm^{-1} in the MEF II spectrum, a shift projected by DFT calculations.

The bands at the lowest energy region, $630\text{--}570\text{ cm}^{-1}$, are related to differences among the forms revealed by vibrational modes involving the N atoms bonded to the aromatic rings. The significant shift from 626 cm^{-1} (MEF I) to 575 cm^{-1} (MEF II), assigned to the $\gamma\text{ N-H}$ in-phase and out-of-phase bending (Scheme 1k and l), can be related to the distinct packing of the molecules in the polymorphs, which constitutes a particular sensitive mode to the molecular conformations. Indeed, as shown in Figure 1, the main difference between the two polymorphs is in the dihedral angle $\theta_2 = \tau(\text{C}_1\text{-N-C}_8\text{-C}_9)$.

The experimental and calculated ^{13}C NMR spectra of the polymorphs are shown in Figure 8; the chemical shift values are reported in Table 4. Kojima et al.⁵³ used solid-state ^{13}C NMR of mefenamic acid only to compare the free molecule and the solid dispersion with the polymer EUDRAGIT. Therefore, no discussion has been done yet to correlate the presence of polymorphism in the NMR characterization of this drug. The presently obtained results (Figure 8a) indicate that the ^{13}C NMR spectrum reported by Kojima et al. can be assigned to the MEF I form (with a 1 ppm shift).

Both NMR spectra shown in Figure 8 are very similar. The theoretical ^{13}C NMR chemical shifts are in the same range of the experimental values. The largest chemical shift observed for MEF I (173 ppm) and MEF II (174 ppm) is assigned to C7, which is in agreement with data reported for the carboxylic group (150–185 ppm).^{21,54} The partial charge obtained using a natural bond orbital (NBO) analysis for C7 can be correlated to this chemical shift;⁵⁵ the electron delocalization at the C7 site is due to the binding of the atoms of high electronegativity in the carboxylic group.

The C1 to C6 and C8 to C13 chemical shifts are in the range of the aromatic compounds with substituents (93–163 ppm). The C11–C13 chemical shifts (approximately 125 ppm) and negative partial charges are very similar. Although C8 and C9–C10 present a slight difference in the chemical shift, the opposite partial charge can be seen due to the atoms bonded to the carbon atoms. The C8 atom bonded to nitrogen, a receptor of electrons, has positive partial charge, while the C9–C10 bonded to the methyl groups, a donor of electrons, presents a negative partial charge.

The chemical shifts of the sp^3 carbon atoms in the methyl groups (C14 and C15) are much smaller than the chemical shifts of the sp^2 carbon atoms in the aromatic ring (C9 and C10). C1 of the benzoic group has a larger chemical shift (150–158 ppm) when compared to C8 (127–143 ppm). Moreover, the C2 (108 ppm) is deshielded in contrast to the C1 (150 ppm) due to the influence of the carboxylic group. The C4 (114–119 ppm) and C6 (110–115 ppm) are at the

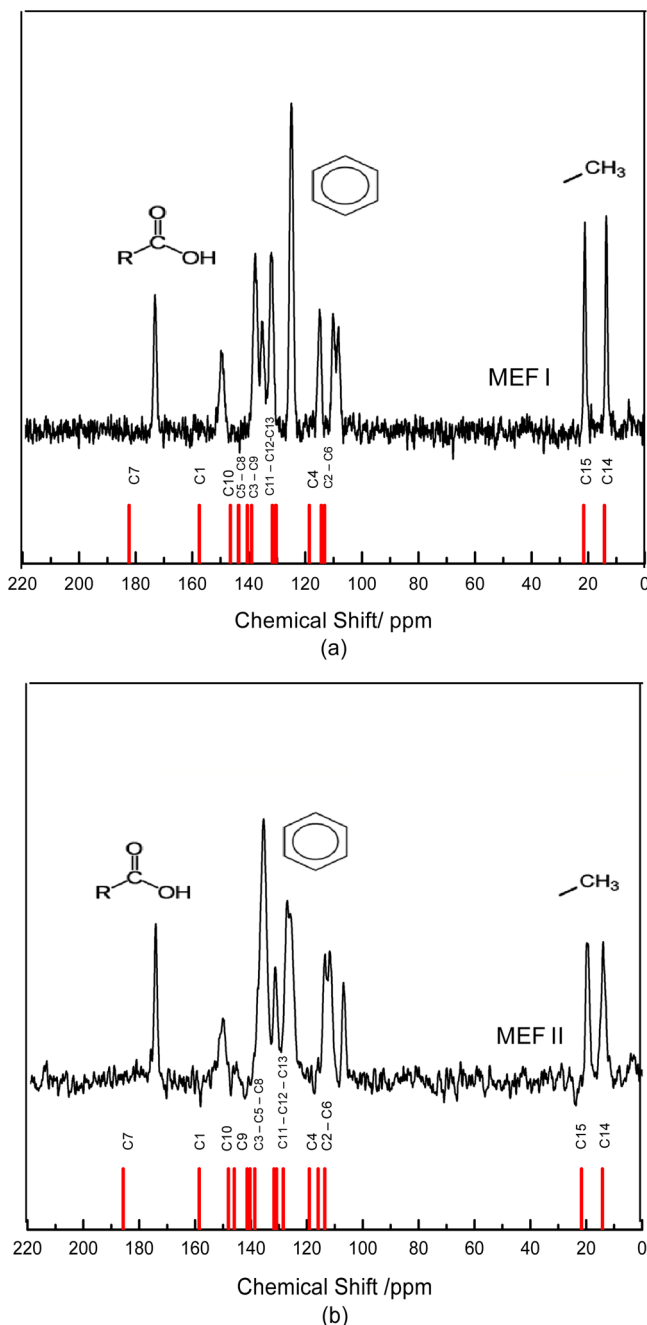


Figure 8. ^{13}C solid-state CP/MAS NMR spectra (black line) and theoretical NMR chemical shifts (red ticks) obtained for MEF I (a) and MEF II (b).

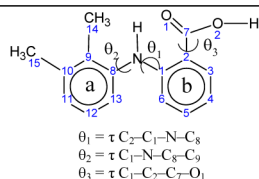
meta position related to the carboxylic group. Consequently, these values are smaller than 127–140 ppm observed for C3 (*ortho*) and C5 (*para*). A remarkable difference between the polymorphs is the chemical shifts of C8 (135.8 and 127.6 ppm) and C9 (139.4 and 143.3 ppm) for MEF I and MEF II, respectively. These carbon atoms are related to the angle θ_2 which characterizes the main structural difference between the two polymorphic forms.

CONCLUSIONS

XRD and TGA-DSC data confirmed the isolation of polymorphs I and II of mefenamic acid. In the solid state, the attribution of the vibrational Raman and IR modes has to

Table 4. Experimental Solid-State ^{13}C CPMAS NMR Chemical Shift (ppm) and Calculated Chemical Shifts for MEF I and MEF II Samples Using the Functional/Basis Set B3LYP/6311+G**

Carbon atom	MEF I		MEF II	
	Calculated	Experimental	Calculated	Experimental
C7	181.53	173.90	181.37	174.88
C1	156.86	149.96	157.94	150.58
C10	145.54	137.83	144.56	136.10
C8	143.54	135.74	142.62	127.58
C5	140.27	135.42	140.29	127.58
C9	139.35	132.48	143.26	131.58
C3	138.97	131.58	138.85	127.58
C11	130.64	125.29	133.39	126.51
C13	129.52	125.29	131.45	126.51
C12	128.93	125.29	131.34	126.51
C4	119.03	115.23	118.61	114.02
C6	115.99	110.50	115.71	112.38
C2	113.22	108.50	112.67	107.40
C15	21.23	21.10	22.04	19.53
C14	14.47	13.51	14.01	14.09



take into account the formation of dimers. Mefenamic acid exhibits conformational polymorphism, and the main difference between them is the θ_2 torsion angle. The significant shift from 626 cm^{-1} (MEF I) to 575 cm^{-1} (MEF II), assigned to the γ N–H in-phase and out-of-phase bending, is sensitive to the molecular conformation and was used as a marker to differentiate the two polymorphs. ^{13}C NMR data showed the distinction between the forms by the peaks related to three groups in the molecule: carboxylic, aromatic ring, and methyl.

The results presented in this work contribute to the better physical chemical characterization of mefenamic acid, a valuable pharmaceutical compound.

AUTHOR INFORMATION

Corresponding Author

*Phone: 55 11 3091-9152. E-mail: vrlconst@iq.usp.br.

Present Address

||(C.M.S.I.) Núcleo de Espectroscopia e Estrutura Molecular, Departamento de Química, Universidade Federal de Juiz de Fora, CEP 36036-900, Juiz de Fora-MG, Brazil.

Notes

The authors declare no competing financial interest.

ACKNOWLEDGMENTS

The authors acknowledge the financial support and fellowships from the Brazilian agencies Fundação de Amparo à Pesquisa do Estado de São Paulo (FAPESP), projects 2011/50318-1 and

2012/12209-9), Conselho Nacional de Desenvolvimento Científico e Tecnológico (CNPq), and Nanobiomed (Nanomedicine Network/CAPES). We also appreciate the support from NAP-NN (Núcleo de Apoio à Pesquisa em Nanossistemas e Nanotecnologia) from Universidade de São Paulo.

REFERENCES

- (1) Brittain, H. G. Polymorphism and Solvatomorphism 2005. *J. Pharm. Sci.* **2005**, *96*, 705–728.
- (2) Saurabh, G.; Kaushal, C. Pharmaceutical Solid Polymorphism in Abbreviated New Drug Application (ANDA) – A Regulatory Perspective. *J. Chem. Pharm. Res.* **2011**, *3*, 6–17.
- (3) Domanska, U.; Pobudkowska, A.; Pelczarska, A. Solubility of Sparingly Soluble Drug Derivatives of Anthranilic Acid. *J. Phys. Chem. B* **2011**, *115*, 2547–2554.
- (4) Hughes, C. E.; Williams, P. A.; Peskett, T. R.; Harris, K. D. M. Exploiting In Situ Solid-State NMR for the Discovery of New Polymorphs During Crystallization Processes. *J. Phys. Chem. Lett.* **2012**, *21*, 3176–3181.
- (5) Center for drug evaluation and research. *Guidance for industry; Abbreviated new drug application (ANDA): Pharmaceutical solid polymorphism chemistry, manufacturing, and controls information*, 2007.
- (6) Gasparin, L.; Ongini, E.; Wenk, G. Non-steroidal Anti-Inflammatory Drugs (NSAIDs) in Alzheimer's Disease: Old and New Mechanisms of Action. *J. Neurochem.* **2004**, *91*, 521–536.
- (7) Zha, S.; Yegnasubramanian, V.; Nelson, W. G.; Isaacs, W. B.; De Marzo, A. M. Cyclooxygenases in Cancer: Progress and Perspective. *Cancer Lett.* **2004**, *215*, 1–20.
- (8) <http://www.medicines.org.uk>, accessed Feb 2014.

- (9) Demertzis, D. K.; Litina, D. H.; Staninska, M.; Primikiri, A.; Kotoglov, C.; Demertzis, M. A. Anti-oxidant, *in vitro*, *in vivo* Anti-Inflammatory Activity and Antiproliferative Activity of Mefenamic Acid and its Metal Complexes with Manganese(II), Cobalt(II), Nickel(II), Copper(II) and Zinc(II). *J. Enzyme Inhib. Med. Chem.* **2009**, *24*, 742–752.
- (10) Hernández, A. D. S.; Salazar, H. R. G.; Galindo, D. A. M.; Hernandez, A. R.; Martinez, R. M.; Esquivel, J. G.; Velazquez, L. L. V.; Rodriguez, L. M. B.; Gómez, F. E.; Martinez, A. R.; et al. Antitumor Effect of Meclofenamic Acid on Human Androgen-independent Prostate Cancer: a Preclinical Evaluation. *Int. Urol. Nephrol.* **2012**, *44*, 471–477.
- (11) Woo, D. H.; Han, I. S.; Jung, G. Mefenamic Acid-induced Apoptosis in Human Liver Cancer Cell-lines through Caspase-3 Pathway. *Life Sci.* **2004**, *24*, 2439–2449.
- (12) Lozano, J. J.; Pouplana, R.; López, M.; Ruiz, J. Conformational Analysis of the Antiinflammatory Fenamates: a Molecular Mechanics and Semiempirical Molecular Orbital Study. *J. Mol. Struct.: THEOCHEM* **1995**, *335*, 215–227.
- (13) Dhanaraj, V.; Vijayan, M. Structural Studies of Analgesics and their Interactions XII. Structure and interactions of anti-inflammatory fenamates: A Concerted Crystallographic and Theoretical Conformational Study. *Acta Crystallogr.* **1988**, *44*, 406–412.
- (14) McConnell, J. F.; Company, F. Z. N-(2,3-Xylyl)anthranilic acid, $C_{15}H_{15}NO_2$, Mefenamic Acid. *Cryst. Struct. Commun.* **1976**, *5*, 861–864.
- (15) Lee, E. H.; Byrn, S. R.; Carvajal, M. T. Additive-induced Metastable Single Crystal of Mefenamic Acid. *Pharm. Res.* **2006**, *23*, 2375–2380.
- (16) Surov, O. A.; Terekhova, I. V.; Bauer-Brandl, A.; Perlovich, G. L. Thermodynamic and Structural Aspects of Some Fenamate Molecular Crystals. *Cryst. Growth Des.* **2009**, *9*, 3265–3272.
- (17) Seethalekshmi, S.; Row, T. N. G. Conformational Polymorphism in a Non-steroidal Anti-inflammatory Drug, Mefenamic Acid. *Cryst. Growth Des.* **2012**, *12*, 4283–4289.
- (18) Romero, S.; Escalera, B.; Bustamante, P. Solubility Behavior of Polymorphs I and II of Mefenamic Acid in Solvent Mixtures. *Int. J. Pharm.* **1999**, *178*, 193–202.
- (19) Gilpin, R. K.; Zhou, W. Infrared Studies of the Thermal Conversion of Mefenamic Acid Between Polymorphic States. *Vib. Spectrosc.* **2005**, *37*, 53–59.
- (20) Chan, H. K.; Doelker, E. Polymorphic Transformation of Some Drugs Under Compression. *Drug Dev. Ind. Pharm.* **1985**, *11*, 315–332.
- (21) Kruszynski, R.; Trzesowska-Kruszynska, A.; Majewski, P.; Łukaszewicz, E.; Majewska, K.; Sierański, T.; Lewiński, B. Structure and Properties of the Sodium, Potassium and Calcium Salts of 2-(2,3-dimethylphenyl)aminobenzoic Acid. *J. Mol. Struct.* **2010**, *970*, 79–89.
- (22) Wolfs, I.; Desseyn, H. O. Modelling the Vibrational Behaviour of the Cyclic Carboxylic Acid Dimer. SQM Force Field of the Formic Acid Dimer. *J. Mol. Struct.: THEOCHEM* **1996**, *360*, 81–97.
- (23) Mikulskiene, B.; Sablinskas, V.; Balevicius, V.; Dikeius, G.; Kimtys, L. Raman and IR Studies of Isomerization and Self-association of β,β' -dichloropivalic Acid. *Vib. Spectrosc.* **1998**, *17*, 163–171.
- (24) Dubis, A. T.; Grabowski, S. J.; Romanowska, D. B.; Misiaszek, T.; Leszczynski, J. Pyrrole-2-carboxylic Acid and its Dimers: Molecular Structure and Vibrational Spectrum. *J. Phys. Chem. A* **2002**, *106*, 10613–10621.
- (25) Balachandran, V.; Karthick, T.; Perumal, S.; Nataraj, A. Vibrational Spectroscopic Studies, Molecular Orbital Calculations and Chemical Reactivity of 6-nitro-m-toluic Acid. *Spectrochim Acta, Part A* **2012**, *92*, 137–147.
- (26) Moreno, J. R. A.; Urena, F. P.; Gonzalez, J. J. L. Conformational Landscape and Hydrogen Bonding in (S)-(-)-perillyc Acid: Experimental VCD, IR, Raman, and Theoretical DFT Studies. *Tetrahedron: Asymmetry* **2012**, *23*, 780–788.
- (27) Yenagi, J.; Shettar, A.; Tonannavar, J. On the Anomalous Vibration Spectra and O-H..N Bond Dictated Structure of 3-fluoroisonicotinic Acid. *Vib. Spectrosc.* **2012**, *63*, 342–349.
- (28) Vueba, M. L.; Pina, M. E.; Carvalho, L. A. E. B. Conformational Stability of Ibuprofen: Assessed by DFT Calculations and Optical Vibrational Spectroscopy. *J. Pharm. Sci.* **2008**, *97*, 845–859.
- (29) Nolasco, M. M.; Amado, A. M.; Claro, P. J. A. R. Effect of Hydrogen Bonding in the Vibrational Spectra of trans-Cinnamic Acid. *J. Raman Spectrosc.* **2009**, *40*, 394–400.
- (30) Kato, F.; Otsuka, M.; Matsuda, Y. Kinetic Study of the Transformation of Mefenamic Acid Polymorphs in Various Solvents and Under High Humidity Conditions. *Int. J. Pharm.* **2006**, *321*, 18–26.
- (31) Umeda, T.; Ohnishi, N.; Yokoyama, T.; Kuroda, T.; Kita, Y.; Kuroda, K.; Tatsumi, E.; Matsuda, Y. A Kinetic Study on the Isothermal Transition of Polymorphic Forms of Tolbutamide and Mefenamic Acid in the Solid State at High Temperatures. *Chem. Pharm. Bull.* **1985**, *33*, 2073–2078.
- (32) Lee, C. T.; Yang, W. T.; Parr, R. G. Development of the Colle-Salvetti Correlation Energy Formula into a Functional of the Electron Density. *Phys. Rev. B* **1988**, *37*, 785–789.
- (33) Becke, A. D. Density-functional Thermochemistry IV: A New Dynamical Correlation Functional and Implications for Exact-exchange Mixing. *Chem. Phys.* **1996**, *104*, 1040–1046.
- (34) Frisch, M. J.; Trucks, G. W.; Schlegel, H. B.; Scuseria, G. E.; Robb, M. A.; Cheeseman, J. R.; Zakrzewski, V. G.; Montgomery, J. A., Jr.; Stratmann, R. E.; Burant, J. C.; et al. *Gaussian 98*, revision A.7; Gaussian, Inc.: Pittsburgh, PA, 1998.
- (35) Foster, J. P.; Weinhold, F. Natural Hybrid Orbitals. *J. Am. Chem. Soc.* **1980**, *102*, 7211–7218.
- (36) Andersson, M. P.; Uvdal, P. New Scale Factors for Harmonic Vibrational Frequencies using the B3LYP Density Functional Method with the Triple- ζ Basis Set 6-311+G(d,p). *J. Phys. Chem. A* **2005**, *109*, 2937–2941.
- (37) Cunha, V. R. R.; Petersen, P. A. D.; Gonçalves, M. B.; Petrilli, H. M.; Taviot-Gueho, C.; Leroux, F.; Temperini, M. L. A.; Constantino, V. R. L. Structural, Spectroscopic (NMR, IR, and Raman), and DFT Investigation of the Self-Assembled Nanostructure of Pravastatin-LDH (Layered Double Hydroxides) Systems. *Chem. Mater.* **2012**, *24*, 1415–1425.
- (38) Tzeli, D.; Theodorakopoulos, G.; Petsalakis, I. D.; Ajami, D.; Rebek, J. Theoretical Study of Hydrogen Bonding in Homodimers and Heterodimers of Amide, Boronic Acid, and Carboxylic Acid, Free and in Encapsulation Complexes. *J. Am. Chem. Soc.* **2011**, *133*, 16977–16985.
- (39) Aguiar, A. J.; Zelmer, J. E. Dissolution Behavior of Polymorphs of Chloramphenicol Palmitate and Mefenamic Acid. *J. Pharm. Sci.* **1969**, *58*, 983–987.
- (40) Adam, A.; Schrimpl, A. L.; Schimidt, P. C. Some Physicochemical Properties of Mefenamic Acid. *Drug Dev. Ind. Pharm.* **2000**, *26*, 477–487.
- (41) Panchagnula, R.; Sundaramurthy, P.; Pillai, O.; Agrawal, S.; Raj, Y. A. Solid-state Characterization of Mefenamic Acid. *J. Pharm. Sci.* **2004**, *93*, 1019–1029.
- (42) Cesur, S.; Gokbel, S. Crystallization of Mefenamic Acid and Polymorphs. *Cryst. Res. Technol.* **2008**, *43*, 720–728.
- (43) Andrews, G. P.; Zhai, H.; Tipping, S.; Jones, D. S. Characterisation of the Thermal, Spectroscopic and Drug Dissolution Properties of Mefenamic Acid and Polyoxyethylene-polyoxypropylene Solid Dispersions. *J. Pharm. Sci.* **2009**, *98*, 4545–4556.
- (44) Otsuka, M.; Nishizawa, J. C.; Shibata, J.; Ito, M. Quantitative Evaluation of Mefenamic Acid Polymorphs by Terahertz-Chemometrics. *J. Pharm. Sci.* **2010**, *99*, 4048–4053.
- (45) Adam, A.; Schrimpl, A. L.; Schimidt, P. C. Some Physicochemical Properties of Mefenamic Acid. *Drug Dev. Ind. Pharm.* **2000**, *26*, 477–487.
- (46) Romero, S.; Bustamante, P.; Escalera, B.; Cirri, M.; Mura, P. Characterization of the Solid Phases of Paracetamol and Fenamates at Equilibrium in Saturated Solutions. *J. Therm. Anal. Calorim.* **2004**, *77*, 541–554.

- (47) Datta, S. S.; Grant, D. J. W. Crystal Structures of Drugs: Advances in Determination, Prediction and Engineering. *Nat. Rev. Drug Discovery* **2004**, *3*, 42–57.
- (48) Jabeen, S.; Dines, T. J.; Leharne, S. A.; Chowdhry, B. Z. Raman and IR Spectroscopic Studies of Fenamates - Conformational Differences in Polymorphs of Flufenamic Acid, Mefenamic Acid and Tolfenamic Acid. *Spectrochim. Acta, Part A* **2012**, *96*, 972–985.
- (49) Gilpin, R. K.; Zhou, W. Infrared Studies of the Polymorphic States of the Fenamates. *J. Pharm. Biomed. Anal.* **2005**, *37*, 509–515.
- (50) Lee, I. S.; Lee, A. Y.; Myerson, A. S. Concomitant Polymorphism in Confined Environment. *Pharm. Res.* **2008**, *25*, 960–968.
- (51) Hongo, K.; Watson, M. A.; Carrera, R. S. S.; Iitaka, T.; Guzik, A. A. Failure of Conventional Density Functionals for the Prediction of Molecular Crystal Polymorphism: A Quantum Monte Carlo Study. *J. Phys. Chem. Lett.* **2010**, *1*, 1789–1794.
- (52) Naumov, V. A.; Tafipol'skii, M. A.; Naumov, A. V.; Samdal, S. Molecular Structure of Diphenylamine by Gas-phase Electron Diffraction and Quantum Chemistry. *Russ. J. Gen. Chem.* **2005**, *75*, 923–932.
- (53) Kojima, T.; Higashi, K.; Suzuki, T.; Tomono, K.; Moribe, K. Stabilization of a Supersaturated Solution of Mefenamic Acid from a Solid Dispersion with EUDRAGIT®EPO. *Pharm. Res.* **2012**, *29*, 2777–2791.
- (54) Silverstein, R. M.; Webster, F. X.; Kiemle, D. J. *Spectrometric Identification of Organic Compounds*, 7th ed.; John Wiley & Sons: New York, 2005; Chapter 4, pp 204–244.
- (55) Reed, A. E.; Curtiss, L. A.; Weinhold, F. Intermolecular interactions from a natural bond orbital, donor-acceptor viewpoint. *Chem. Rev.* **1988**, *88*, 899–926.